INVERSE SYNTHETIC APERTURE RADAR (ISAR) IMAGING : A NOVEL FINE RANGE PROFILE ALIGNMENT METHOD FOR AIR TARGET SLANT RANGE ROTATIONAL MOTION COMPENSATION

E. D. Kallitsis, A. V. Karakasiliotis and P. V. Frangos
National Technical University of Athens,
School of Electrical and Computer Engineering,
9, Iroon Polytechniou Str., 157 73 Zografou, Athens, Greece
e-mail: ekalorama@gmail.com, anastasiskarak@yahoo.gr,
pfrangos@central.ntua.gr

Abstract

In this paper we propose the use of a super-resolution decimative spectrum estimation (DESED) method for highly accurate estimation of the slant-range positions of the target scattering centers. Based on these position estimates, we develop a novel slant-range rotational compensation (SRRC) method. The proposed decimative spectrum estimation based SRRC technique achieves fine range alignment, in terms of fractional range bin correction, and constitutes the first step towards significant de-blurring of the final ISAR image. The proposed method is validated with synthetic ISAR data under realistic simulation scenarios, for both uniform and non-uniform rotational motion.

Keywords : Inverse Synthetic Aperture Radar (ISAR), Range Profile Alignment, Air Target Rotational Motion Compensation, Super-resolution Decimative Spectrum Estimation Method (DESED), Coherent Processing Interval (CPI).

1. INTRODUCTION

Inverse synthetic aperture radar (ISAR) is a radar technique to obtain a high resolution image of a moving target. Usually, a wideband transmitted waveform is used to obtain high slant-range resolution, whereas cross-range resolution depends on target aspect angle variation during the coherent processing interval (CPI) [1]. The conventional assumption of relatively small aspect angle variation during CPI is vitiated for small, rapidly maneuvering targets (i.e. fighter aircrafts) [2]. In the current scenario of high-range resolution radar and non-cooperative target, the rotational motion parameters of the target are unknown and migration through resolution cells (MTRC) is apparent in the obtained ISAR images, in both slant-range and cross-range direction [1]-[4]. Target motion may be divided into a translational component and a

rotational component [2]. The first one is further decomposed into a radial and a tangential component, whereas the second one has three attitude components: yaw, pitch and roll. On the one hand, the radial component of the translational motion [that is, the component along the line-of-sight (LOS)] is undesired, because it does not induce variation of the target aspect angle, i.e. it does not generate Doppler gradient among target scatterers situated in the same range bin. Furthermore, this component causes significant blurring in ISAR images.

On the other hand, the rest of motion components may produce the desired Doppler gradient among scatterers, hence obtaining two - dimensional information. It is true that the rotational motion (and the tangential component of the translational motion), may also generate blurring effects on the image (MTRC), but they are of minor importance compared to the blurring caused by the radial component of the translational motion, which must always be compensated [3]. Conventional methods for translational motion compensation [1], [2] mostly follow two steps: (i) range tracking (coarse range bin alignment) and Doppler tracking (fine phase correction with respect to a prominent scatterer). Range tracking can keep scatterers in their range cells, while Doppler tracking keeps Doppler frequency shift of each scatterer constant during CPI.

Range tracking can be performed by a cross-correlation method that finds misaligned range cells with respect to a reference range profile and then performs range alignment for all other range profiles. Cross-correlation allows for integer range bin correction, thus it has no capability of compensating misalignments less than slant-range resolution. Even if zero padding is performed before Fast Fourier transform (FFT) is applied to derive range profiles, cross-correlation based range alignment method can only estimate more accurately the average slant-range migration of the target as a whole and not the migration of each scatterer individually. On the other hand, Doppler tracking is performed through a phase compensation procedure, usually including three steps: (i) searching for one or several reference range cells by using a criterion such as minimum variance, (ii) taking conjugate phase at the reference range cells, and (iii) making phase correction for all range cells using the conjugate phase.

In this paper, we develop a novel fine range alignment method that can very accurately compensate for different slant-range migrations of individual scatterers of a

rotating target. In Section 2, we start with the mathematical description of the ISAR problem, simply examining rotational motion migration phenomena (slant-range and cross-range migration). Section 3 presents the proposed range alignment method that is based on range position estimates derived by applying a super-resolution decimative spectrum estimation method, namely DESED [5], on raw ISAR data. These range estimates are applied to raw data as compensating phase terms, separately for each scatterer, and the obtained per scatterer range profiles are combined together to produce finely aligned overall range profiles. In Section 4, we present simulation results from synthetic ISAR data for both uniform and non-uniform rotational motion. Conclusions are drawn in the last section, pointing out novelty and validity of the proposed method.

2. MATHEMATICAL DESCRIPTION

Figure 1 shows the position of a rotating scatterer at the initial instant (p_0) and at slow-time instant τ. Translational motion compensation is assumed to be completed and ISAR image artifacts induced by rotational motion have to be compensated. Consequently, the rotation center does not change its position during the CPI. R_0 is the distance from the radar to the rotation center. The following calculations divide the MTRC into migration in slant-range and cross-range [6].

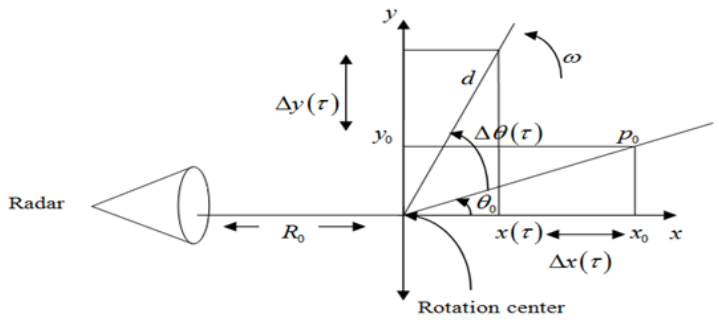

Fig. 1: ISAR scenario with a rotating scatterer

$\Delta x(\tau)$ is the rotation-induced slant-range migration of the scatterer and has the expression $\Delta x(\tau) = x(\tau) - x_0$, where $x(\tau) = d\cos(\theta_0 + \Delta\theta(\tau))$ and $x_0 = d\cos(\theta_0)$.

Thus

$$\Delta x(\tau) = d\left[\cos(\theta_0)\cos(\Delta\theta(\tau)) - \sin(\theta_0)\sin(\Delta\theta(\tau)) - \cos(\theta_0)\right] \quad (1)$$

Assuming that $\Delta\theta(\tau)$ is not very large, the following Taylor series approximations are applicable

$$\sin(\Delta\theta(\tau)) \approx \Delta\theta(\tau)$$

$$\cos(\Delta\theta(\tau)) \approx 1 - \frac{(\Delta\theta(\tau))^2}{2} \quad (2)$$

Taking second order term into account, the following equation describes slant-range migration

$$\begin{aligned} \Delta x(\tau) &= -d\cos(\theta_0)\frac{(\Delta\theta(\tau))^2}{2} - d\sin(\theta_0)\Delta\theta(\tau) \\ &= -y_0\Delta\theta(\tau) - x_0\frac{(\Delta\theta(\tau))^2}{2} \end{aligned} \quad (3)$$

With respect to cross-range, the received signal phase for the rotating scatterer at instant τ is $\varphi(\tau) = \frac{4\pi}{\lambda}R(\tau)$, where λ is the wavelength and $R(\tau)$ is the range from the radar to the scatterer.

Since $R(\tau)$ can be approximated as

$$R(\tau) = R_0 + x(\tau) \quad (4)$$

where $x(\tau) = d\cos(\theta_0 + \Delta\theta(\tau))$

$$\begin{aligned} &= d\left[\cos(\theta_0)\cos(\Delta\theta(\tau)) - \sin(\theta_0)\sin(\Delta\theta(\tau))\right] \\ &= x_0\cos(\Delta\theta(\tau)) - y_0\sin(\Delta\theta(\tau)) \end{aligned}$$

Using the approximations of Eq. (2), without ignoring the term $x_0 \frac{\left(\Delta\theta(\tau)\right)^2}{2}$, we derive the phase expression related to cross-range migration

$$\varphi(r) = \frac{4\pi}{\lambda}\left[R_0 + x_0 - y_0\Delta\theta(\tau) - x_0 \frac{\left(\Delta\theta(\tau)\right)^2}{2} \right] \tag{5}$$

SRRC (slant-range rotational compensation) corrects the slant-range migration in induced by rotational motion, as expressed in Eq. (3). The contribution of both slant-range and cross-range to the range misalignment of the obtained ISAR images becomes obvious through the following figure. Simple target geometry of five scatterers is examined in this paper as a proof of concept for the proposed range alignment method. Taking a closer look to the ISAR images of Fig. 2, the significant slant-range migration of the "wing" scatterers $\left(|y_0| > 0\right)$ is apparent, while the "fuselage" scatterers $\left(y_0 = 0\right)$ exhibit quite small range shift, not to mention zero shift for the center of rotation. Equation (3) provides valuable insight into the expected range migration of each scatterer.

On the other hand, CRRC (cross-range rotational compensation) compensates for the last phase term of equation (5) which is associated with the ISAR image blurring. In this paper, it is pre-assumed that the constant distance related phase terms of equation (5) are removed through a translational motion compensation technique [1], [3]. Future research effort is oriented towards a novel CRRC method in view of a combination with the proposed SRRC method [7], [8].

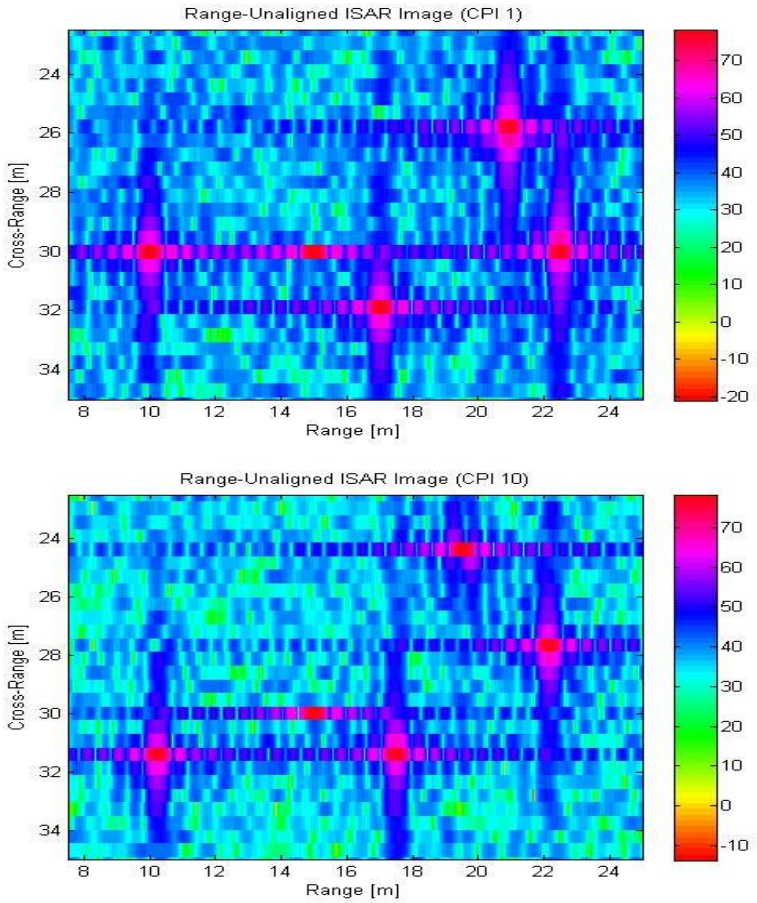

Fig. 2: Slant-range migration induced by uniform rotational motion

3. PROPOSED RANGE ALIGNMENT METHOD

Super-resolution spectrum or frequency estimation techniques have been studied extensively over the past 3 decades from the signal processing community. Amongst their applications radar imaging has been a very important one [9]-[11]. Decimative spectrum estimation methods have also attracted research interest because of their inherent frequency resolution improvement, achieved via decimation of the data sequence under spectral analysis.

In [5], the use of a decimative frequency estimation technique, namely DESED, is proposed for estimating the range positions of target scatterers. Belonging to the wide class of parametric spectrum estimation methods, DESED is applied for a specific order, equal to the number of prominent scatterers, and for a specific decimation factor (D), determined empirically with respect to the available data length.

In this paper, we apply DESED to two-dimensional raw synthetic data, which are

generated by a MATLAB program simulating the classical ISAR geometry with a rotating target consisting of a specific number of point scatterers. In order to derive consistent range estimates from DESED, we need to provide the method with a correct model order (signal model is considered to be a sum of damped exponentials). Order selection is a non-trivial task in parametric spectral analysis [12]. For a radar imaging application, a scattering center extraction method [13], [14] can be employed to estimate accurately the model order for the applied spectrum estimation technique, also giving useful information for the initial range positions of the scattering centers. For simulation purposes in the present study, a trivial peak search algorithm finds the initial range positions, based on the first few range profiles. Alternatively, we use the DESED range estimates averaged over the first few bursts. By taking into account that the rotation center of the target will always be present at the center of the unambiguous range window, we can compute the initial range positions by utilizing DESED estimates.

Analytical mathematical description of DESED method is provided in [5]. The DESED based frequency estimates are translated to range estimates by relating the ISAR signal model to the conventional damped exponentials model. In the proposed approach, we exploit DESED's accuracy and robustness to noise and use the obtained range estimates to calculate the misalignment between range profiles. Each raw data burst is analyzed through DESED. The range estimates for the first burst serve as reference estimates to compute the range migration of each scatterer from burst to burst (slow time). Averaging the range estimates for the first few bursts is an alternative effective way to derive reference estimates in case of low signal-to-noise ratio (SNR).

As shown in Fig. 2 and explained through Eq. (3), each scatterer behaves differently with respect to slant-range and cross-range migration during the imaging integration time (one or more CPIs). For the simple target examined in this paper, we observe in Fig. 2 that the two "wing" scatterers move towards each other in slant-range as the target rotates counter-clockwise. This very important detail is missed by conventional range alignment techniques referring to slant-range migration induced by translational motion.

Throughout this paper we name the amount of range misalignment with respect to the reference range estimates as *normalized range migration*. This amount differs for

each scatterer and is expressed as an integer number of fine range bins. One *fine range bin* unit is a fraction of range resolution ΔR_s (range cell or bin). Fractional range bin correction [15] is achieved via zero-padding each raw data burst by a factor M_{zpd}, before performing FFT based range compression. Thus, one fine range bin unit equals to $\frac{\Delta r_s}{M_{zpd}}$ and the obtained *fine range profile* data length is $M \cdot M_{zpd}$, where M is the raw data burst length.

Once DESED is applied to the current burst and the estimated range misalignments of all scatterers are derived, an aligned range profile has to be formed. The proposed SRRC algorithm consists of four steps with DESED based range estimation being the fundamental one. The block diagram of Fig. 3 presents the basic steps towards fine range alignment. Blocks enclosed by the red dashed box are associated with per scatterer processing, in contrast to per burst processing.

The second step of the proposed SRRC methodology is the individual range shift application, referring to the estimated range migration of each scatterer. Symbolizing DESED order as p and the range estimate of i-th scatterer for the k-th burst as $\hat{r}_i(k)$, the corresponding normalized range migration is computed by

$$\Delta\hat{r}_i(k) = round\left(\frac{\hat{r}_i(k) - \hat{r}_i(o)}{\left\lceil \frac{\Delta r_s}{M_{zpd}} \right\rceil} \right), \quad i = \overline{1, p} \tag{6}$$

where p is DESED order, equal to the number of prominent scatterers ($p = 5$), and i is an index for scatterers (the bar above the symbols shows the values which index i takes).

Utilizing the inherent FFT property of frequency shift, p phase shifted versions of the k-th burst are generated by multiplying it with the term $\exp\left[-j \frac{2\pi}{\left\lceil M \cdot M_{zpd} \right\rceil} (m-1) \Delta\hat{r}_i(k) \right]$ where $m = \overline{1, M}$. In this way, we compensate for the individual range misalignment of each scatterer.

The phase shifted versions of each raw data burst are then transformed through FFT (with zero-padding) into properly range shifted versions of the corresponding

range profile. This is the third step of the proposed SRRC algorithm, named individual fine range profile computation.

The final step is the overall fine range profile synthesis, where the individual fine range profiles are combined into an overall one. First, we construct a mask around the estimated initial range position of the i-th scatterer and we retain the corresponding samples from the i-th fine range profile. The mask length is proportional to the zero-padding factor M_{zpd} and, from a signal processing perspective, it is useful to employ a window function with variable roll-off factor, especially for closely spaced scatterers. The masking procedure is repeated for all p scatterers. Secondly, we detect the "shared regions" between scatterers, again based on their initial positions. The corresponding samples from the f_0 p individual range profiles are averaged in order to compute the contribution of "shared regions" to the overall fine range profile. Azimuth compression through FFT is performed after the fine range alignment procedure to obtain the range-aligned ISAR image.

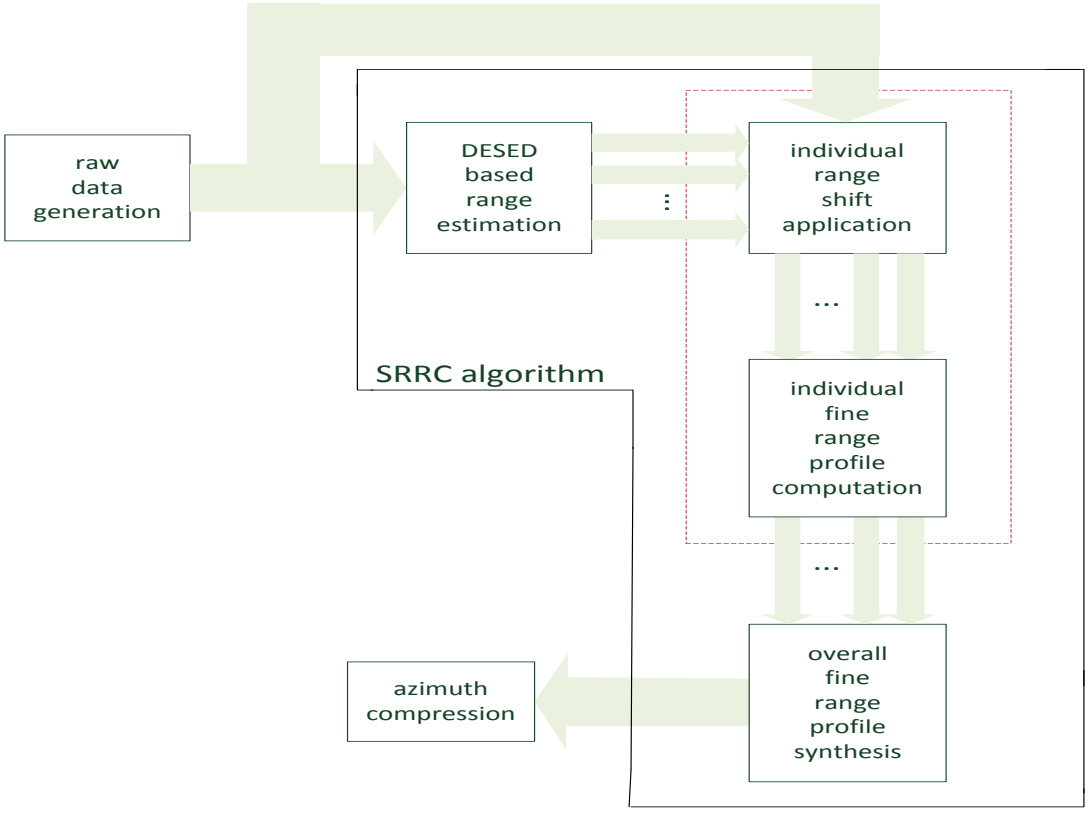

Fig. 3: SRRC algorithm

4. SIMULATION RESULTS

Raw ISAR data for the target of Fig. 4 are generated through MATLAB simulation, based on the signal model presented in [7]. The math formulas for raw data and rotational motion simulation are the following

$$x(m,n)=\sum_{k=1}^{d} s_k \exp\left[-j\frac{4\pi}{c} f_m\left(x_k\cos(\theta_n)-y_k\sin(\theta_n)\right)\right]+u(m,n)$$

$$\theta_n=\theta_0+\omega t_n+\frac{1}{2}\gamma\left(t_n-t_{start}\right)^2 \tag{7}$$

where d the number of scatterers; s_k the scattering intensity of k-th point scatterer; (x_k, y_k) the Cartesian coordinates of k-th point scatterer, with respect to the radar position; m the stepped frequency index $\left(m=\overline{1,M}\right)$ and n the burst index $\left(n=\overline{1, N\cdot N_{CPI}}\right)$ for a number of simulated CPIs (N_{CPI}); N the number of bursts during one CPI; $u(m,n)$ the two-dimensional additive white Gaussian noise component, with simulated SNR equal to 10dB; θ_0 the initial aspect angle of the target, assumed to be at a distance of 10 Km; ω the constant angular velocity; γ the angular acceleration, which is zero for uniform rotation; t_{start} the time instant (as an integer multiple of burst duration) at which an angular acceleration period begins.

Table 1 presents the aforementioned simulation parameters, as following :

Table 1: ISAR simulation parameters

Parameter	**Value [units]**
initial carrier frequency, f_0	10 $\left[GH_z\right]$
range resolution, Δr_s	0.46875 $\left[m\right]$
cross-range resolution, Δr_c	0.47244 $\left[m\right]$
radar bandwidth, B	320 $\left[GH_z\right]$
number of frequencies, M	64
frequency step, Δf	5 $\left[MH_z\right]$
pulse repetition frequency, PRF	15 $\left[KH_z\right]$
burst duration, T_b	4.266 $\left[m\sec\right]$
coherent processing interval, CPI	0.546 $\left[\sec\right]$
number of bursts, N	128
number of CPIs, N_{CPI}	10
angular velocity, ω	0.0586 $\left[rad/\sec\right]$
angular acceleration, γ	0.64 $\left[rad/\sec^2\right]$
model order, p	5
decimation factor, D	2
Zero- padding factor, M_{zpd}	32

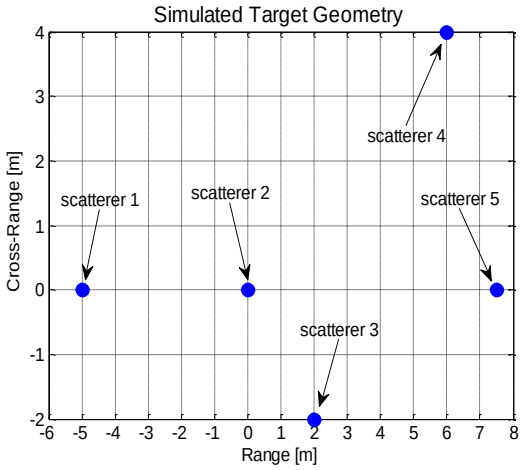

Fig. 4: Simple target geometry with five scatterers

The rotational motion evolution over 10 CPIs simulated in case of uniform and non-uniform rotation is depicted in the next two figures respectively. The latter profile includes angular acceleration within the 4th and the 8th CPI, with smoothed transition from uniform to non-uniform rotation periods.

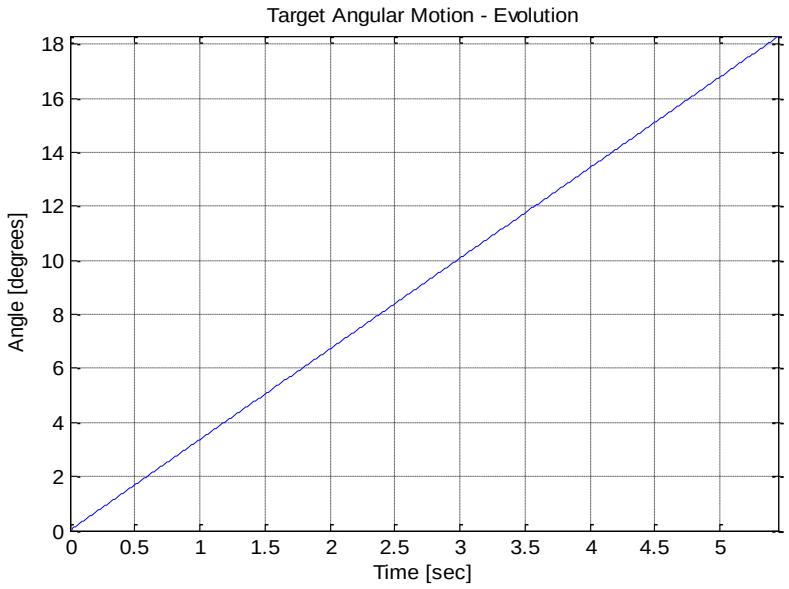

Fig. 5: Uniform rotational motion profile

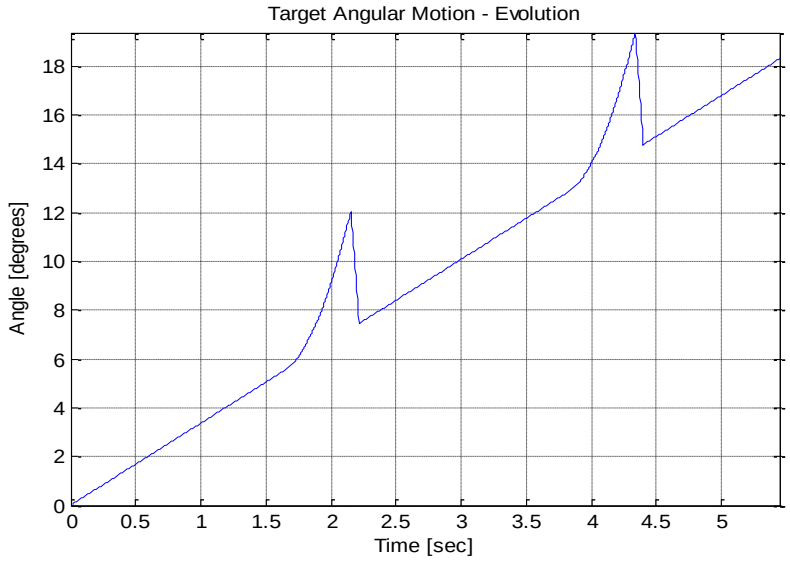

Fig. 6: Non-uniform rotational motion profile

The DESED based range estimates for each scatterer (as noted in Fig. 4) are presented in Figs. 7 and 8 for both simulation scenarios. The variation in terms of fine range bin units is attributed to noise and can be smoothed out by a moving average filter of small length (i.e. 10-20 bursts). As expected, the "wing" scatterers (scatterers 3 and 4) exhibit significant slant-range migration compared to other scatterers, with scatterer 4 migrating by more than 3 range bins during the simulated time. In Fig. 8, the effect of non-uniform rotation is obvious in the range estimate of each scatterer. The similarity of the profile of Fig. 6 with the range estimate of scatterer 4 (at the wing edge) is evident and can be easily explained through Eq. (3).

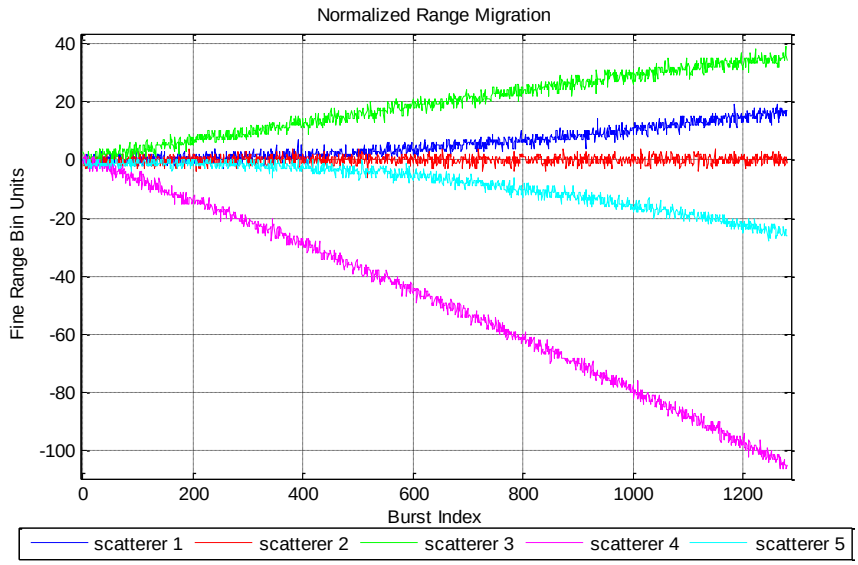

Fig. 7: Normalized range migration of each scatterer for uniform rotation

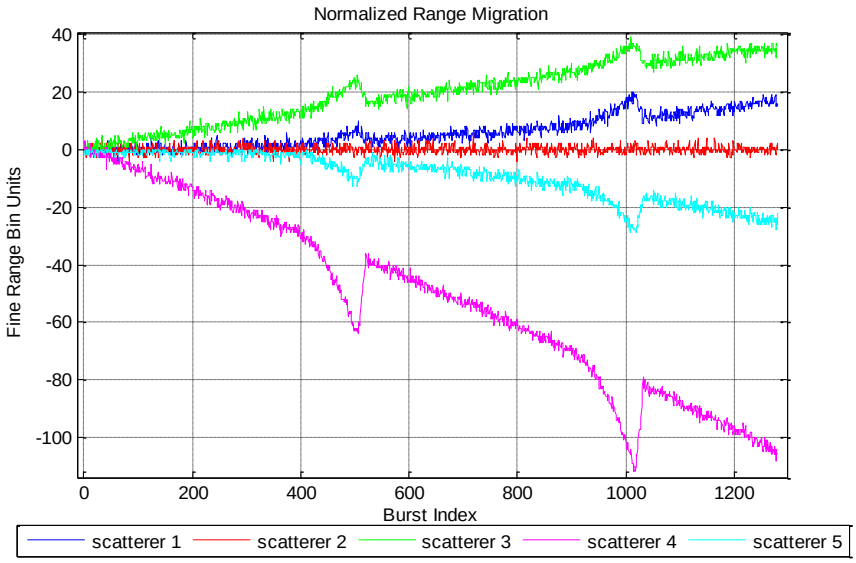

Fig. 8: Normalized range migration of each scatterer for non-uniform rotation

Since DESED provides very accurate and robust to noise range estimates, the proposed range alignment method is expected to produce very well aligned range profiles. In Figs. 9(b) and 10(b), the range alignment is noticeable, as well as the considerable sidelobe reduction within "shared regions" between scatterers.

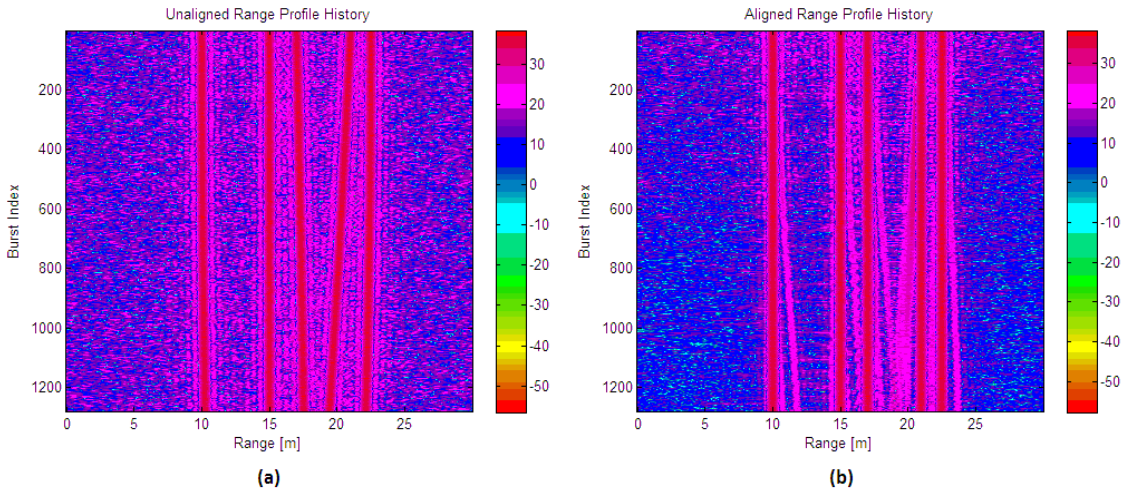

Fig. 9: Range profile history before (a) and after (b) the proposed range alignment method for uniform rotation

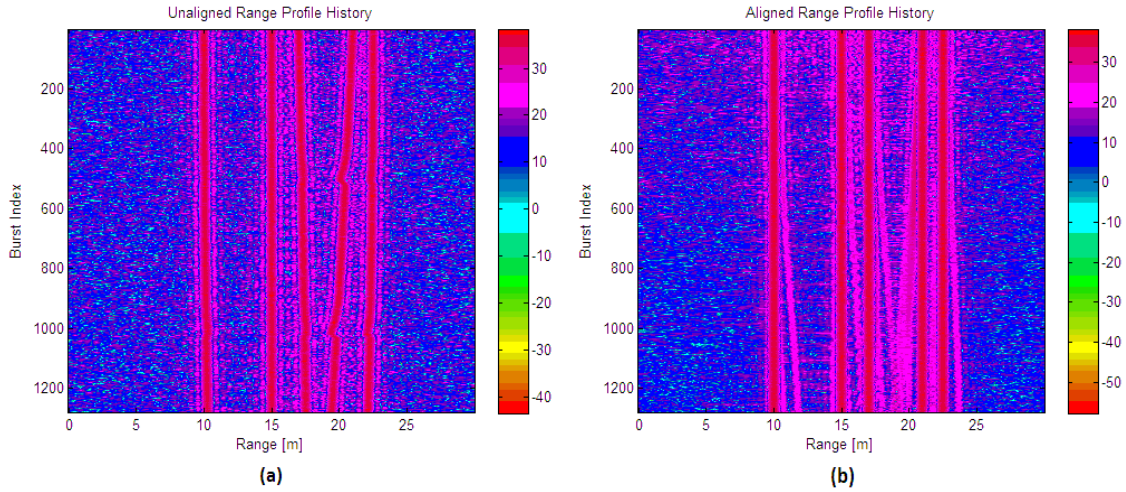

Fig. 10: Range profile history before (a) and after (b) the proposed range alignment method for non-uniform rotation

The focusing effect of the proposed range alignment method can also be verified by examining carefully the obtained ISAR images before and after its application. Figs. 11 and 12 show this effect clearly in range direction for uniform and non-uniform rotation respectively. Furthermore, the entropy values of the power normalized ISAR images [16], shown in Figs. 13 and 14, strongly indicate the focusing improvement after fine range alignment.

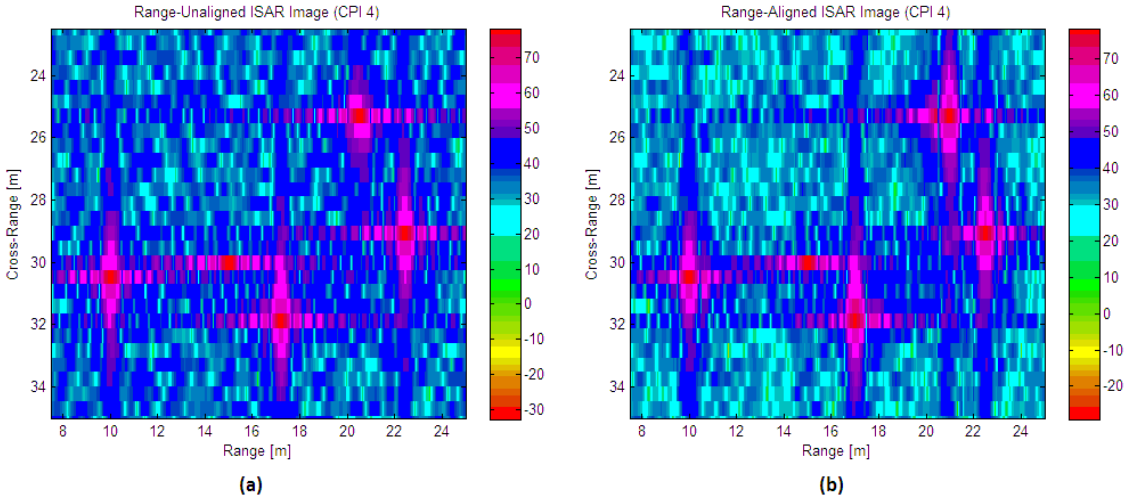

Fig. 11: ISAR images before (a) and after (b) the proposed range alignment method for uniform rotation

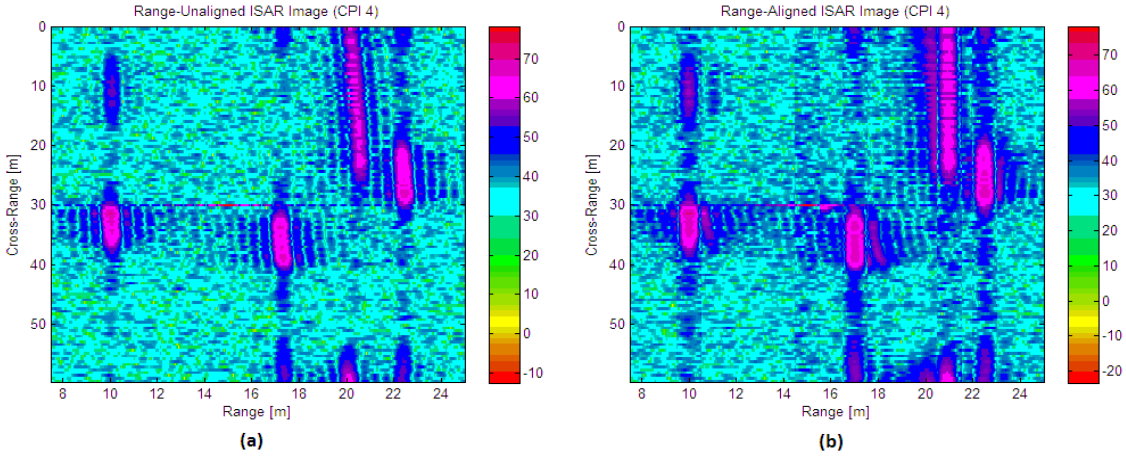

Fig. 12: ISAR images before (a) and after (b) the proposed range alignment method for non-uniform rotation

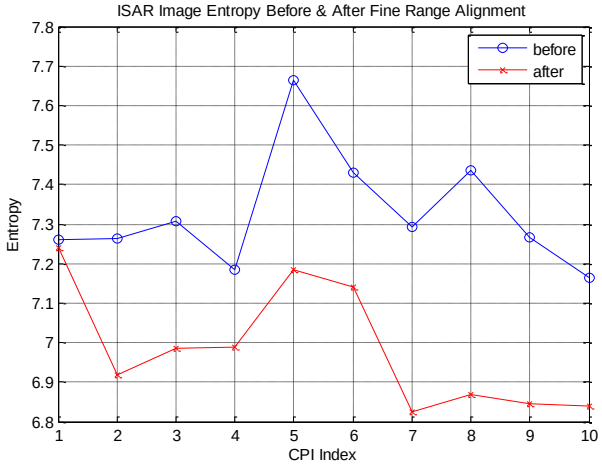

Fig. 13: ISAR image entropy before and after the proposed range alignment method for uniform rotation

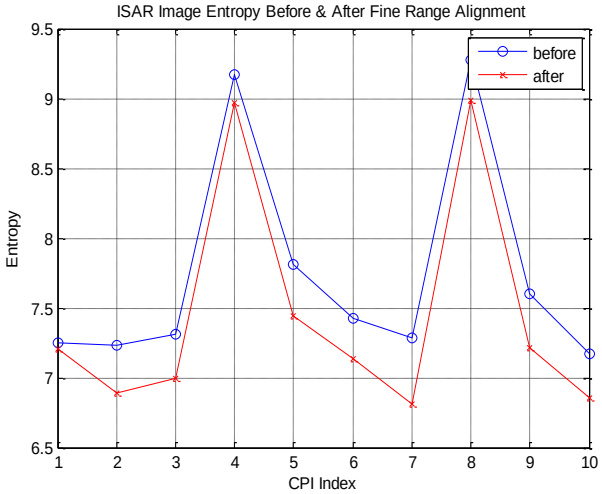

Fig. 14: ISAR image entropy before and after the proposed range alignment method for non-uniform rotation

5. CONCLUSIONS

In this paper we presented a novel slant-range rotational compensation method with application to ISAR imaging. This method is based on super-resolution decimative spectrum estimation for accurate range position estimates. Compared to conventional range alignment methods, our method is capable of fractional range bin correction and takes into account the different slant-range migration of each scatterer. The effectiveness of the proposed range alignment method is proven through extensive ISAR simulations for both uniform and non-uniform air – target rotation, looking into the range profile history, the obtained ISAR images and the corresponding entropy values before and after the application of the proposed methodology.

REFERENCES

[1] D. Wehner, High-Resolution Radar, London, Artech House, 2nd edition, 1995.

[2] V. Chen, and H. Ling, Time-Frequency Transforms for Radar Imaging and Signal Analysis, London, Artech House, 2002.

[3] J. Son, G. Thomas, and B. Flores, Range-Doppler Radar Imaging and Motion Compensation, Artech House, 2001.

[4] G. Lu, and Z. Bao, "Compensation of scatterer migration through resolution cell in inverse synthetic aperture radar imaging", IEE Proc. Radar, Sonar and Navigation, Vol. 147 (2), pp. 80-85, Apr. 2000.

[5] A. Karakasiliotis, and P. Frangos, "Decimative Spectrum Estimation Method for High-Resolution Radar Parameter Estimates," Proc. 5th International Symposium on Communications, Networks and Digital Signal Processing (CSNDSP 2006), Patras, Greece, July 2006.

[6] J. Munoz-Ferreras and F. Perez-Martinez, "Uniform rotational motion compensation for inverse synthetic aperture radar with non-cooperative targets", IET Radar, Sonar and Navigation, Vol. 2 (1), pp. 25-34, Feb. 2008.

[7] E. Kallitsis, A. Karakasiliotis, G. Boultadakis, and P. Frangos, "A Fully Automatic Autofocusing Algorithm for Post-processing ISAR Imaging based on Image Entropy Minimization", Electronics and Electrical Engineering Journal, T121 Signal Technology, No. 4 (110), pp.125-130, Apr. 2011.

[8] E. Kallitsis, A. Karakasiliotis, and P. Frangos, "Combination of range alignment technique with autofocusing post-processing algorithm for ISAR image optimization", International Conference on 'Communications, Electromagnetics and Medical Applications' (CEMA'11), Sofia, Bulgaria, Oct. 2011.

[9] A. Karakasiliotis, and P. Frangos, "Comparison of Several Spectral Estimation Methods for Application to ISAR Imaging," Proc. RTO SET 080 International Symposium on 'Target Identification and Recognition using RF Systems', Oslo, Norway, 11-13 October 2004.

[10] S. DeGraaf, "SAR imaging via modern 2-D spectral estimation methods", IEEE Transactions on Image Processing, Vol. 7 (5), pp.729-761, May 1998.

[11] E. Corral, G. Thomas, and B. Flores, "Effects of using superresolution techniques in ISAR imagery", Proc. CCECE 2002, Vol. 1, pp. 353-357, 2002.

[12] P. Stoica, and Y. Selen, "Model-order selection: a review of information criterion rules", IEEE Signal Processing Magazine, Vol. 21 (4), pp. 36-47, July 2004.

[13] K.-T. Kim, and H.-T. Kim, "Two-dimensional scattering center extraction based on multiple elastic modules network", IEEE Transactions on Antennas and Propagation, Vol.51 (4), pp. 848-861, Apr. 2003.

[14] Y. Wang, J. Chen, and Z. Liu, "Two-dimensional scattering center extraction using super-resolution techniques [Inverse SAR applications]", International Symposium of IEEE Antennas and Propagation Society, Vol. 2, pp. 2091- 2094, June 2004.

[15] J. Munoz-Ferreras, and F. Perez-Martinez, "Sub-integer Range-Bin Alignment Method for ISAR Imaging of Noncooperative Targets", EURASIP Journal on Advances in Signal Processing-Special Issue on Advanced Image Processing for Defense and Security Applications, Vol. 2010, pp. 1-16, Feb. 2010.

[16] A. Karakasiliotis, A. Lazarov, G. Boultadakis, G. Kalognomos and P. Frangos, "Two-dimensional ISAR Model and Image Reconstruction with Stepped Frequency Modulated Signal", IET Signal Processing, Vol. 2 (3), pp. 277-290, Sept. 2008.